

ANALYTICAL INVESTIGATION AND PARAMETRIC STUDY OF LATERAL IMPACT BEHAVIOR OF PRESSURIZED PIPELINES AND INFLUENCE OF INTERNAL PRESSURE**Yangqing Dou**Department of Mechanical Engineering
Mississippi State University
Mississippi State, MS 39762, USA
yd120@me.msstate.edu**Yucheng Liu**Department of Mechanical Engineering
Mississippi State University
Mississippi State, MS 39762, USA
liu@me.msstate.edu**ABSTRACT**

This paper provides a combined computational and analytical study to investigate the lateral impact behavior of pressurized pipelines and inspect all the parameters such as the outside diameter and internal pressure affects such behavior. In this study, quartic polynomial functions are applied to formulate the maximum crushing force (F), maximum permanent displacement (W), and absorbed energy (E) of the pressurized pipelines during the impact problem. The effects of the diameter and pressure on F, W, and E are therefore illustrated through analyzing those functions. Response surfaces are also plotted based on the generated quartic polynomial functions and the quality (accuracy) of those functions are verified through several techniques.

Keywords: pressurized pipeline, quartic polynomial, parametric study, FEA, response surface method

INTRODUCTION

The authors have conducted a computational study to thoroughly investigate lateral impact behavior of pressurized pipelines and inspect effects of internal pressure and outside diameter of the pipelines on their impact responses. 72 impact simulations were carried out using 3D dynamic nonlinear finite element analysis (FEA) through LS-DYNA to predict the impact response of mild steel pipelines with different diameters and internal pressure levels, which subjected to lateral struck at mid-span and one quarter span positions. The obtained computational results were verified by comparing with some

published experimental results. Based on the results achieved from the preliminary analysis, one objective of this study is to employ numerical methods to establish analytical models to numerically show how the impact parameters (internal pressure and outside diameter) affect the impact response of the pipelines during low-speed lateral impact.

PROBLEM DESCRIPTION AND FEA RESULTS

In preliminary computer simulations, a rigid indenter impacted a number of pressurized pipelines at the mid-span position and the one quarter span position. The pressurized pipes were made from seamless cold drawn mild steel with outside diameters of 22, 42, 60, 80, 100, and 120 mm with a fixed ratio of $2L/D = 10$, where $2L$ is the distance between the two supports and D is the outside diameter. The selected ratio of $2L/D = 10$ is currently being used in most research laboratory and industry plant as the largest unsupported pipe length ratio [1]. The cold worked mild steel pipes have a 2mm wall thickness, and the mechanical properties in the axial direction of the pipe are: static uniaxial yield stress $\sigma_y = 663$ MPa, static ultimate tensile stress $\sigma_u = 823$ MPa, and static uniaxial rupture strain $\epsilon_r = 6 \sim 7\%$. In this study, the internal pressure p varies from 0 to 150 bar. Specifically, 6 different pressures, 0, 30, 60, 90, 120, 150 bar were applied on inner surface of the pipelines separately in order to achieve a complete understanding of how the internal pressure affects the lateral impact behavior of the pipelines.

In order to simulate those impact tests, 72 FEA models were created along with appropriate boundary, loading, and initial conditions. The generated FEA models include 1000 to

more than 25,000 shell elements. Figs. 1 and 2 present two impact scenarios, where the indenter impacted a pipeline model with outside diameter of 60 mm and internal pressure of 60 bar at its center and one quarter span, respectively.

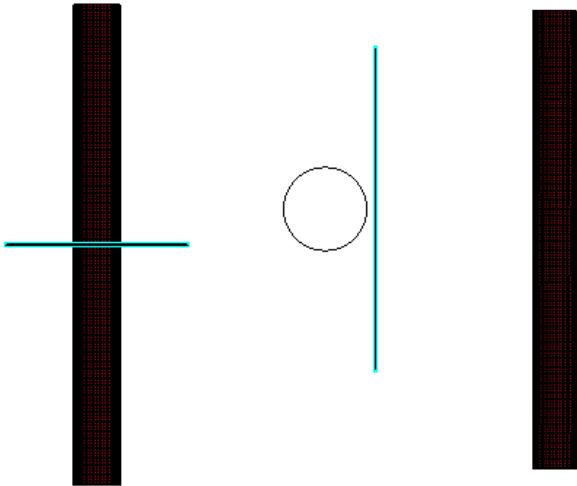


Fig. 1. FEA model showing an indenter impacts on center of a pressurized pipeline

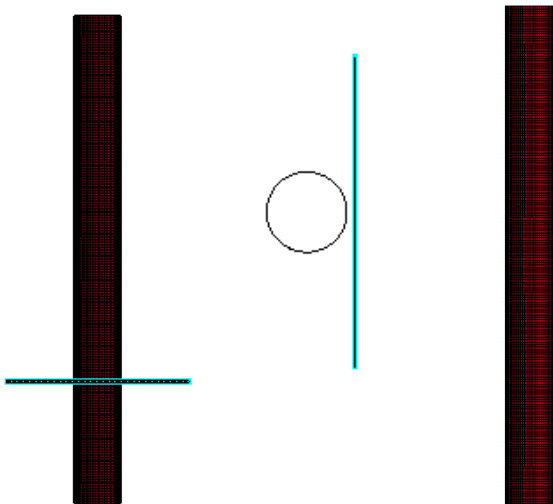


Fig 2. FEA model showing an indenter impacts on one quarter of a pressurized pipeline

After the impact simulations, important FEA results (maximum impact force F, permanent displacement W, and absorbed energy E) were collected and tabulated in Tables 1 and 2 for pipeline models which were struck at middle and one quarter span position, respectively.

No.	D (mm)	p (bar)	W (mm)	F (kN)	E (kJ)
-----	--------	---------	--------	--------	--------

No.	D (mm)	p (bar)	W (mm)	F (kN)	E (kJ)
1	22	0	34.31	47.14	0.83
2	22	30	34.26	47.42	0.83
3	22	60	34.21	47.45	0.83
4	22	90	34.15	47.64	0.83
5	22	120	34.06	47.77	0.83
6	22	150	33.98	47.86	0.83
7	42	0	24.60	50.09	0.78
8	42	30	24.08	51.00	0.77
9	42	60	23.70	51.89	0.77
10	42	90	23.31	52.36	0.77
11	42	120	21.31	52.39	0.77
12	42	150	20.61	52.75	0.76
13	60	0	18.05	56.80	0.71
14	60	30	16.05	59.45	0.69
15	60	60	14.71	61.80	0.67
16	60	90	13.59	64.35	0.66
17	60	120	12.83	65.61	0.65
18	60	150	12.07	67.68	0.64
19	80	0	16.83	58.37	0.65
20	80	30	12.45	64.18	0.59
21	80	60	10.42	69.80	0.56
22	80	90	8.98	74.10	0.53
23	80	120	8.36	76.16	0.52
24	80	150	7.62	76.19	0.51
25	100	0	15.90	59.30	0.61
26	100	30	10.05	68.00	0.51
27	100	60	7.60	74.68	0.50
28	100	90	6.56	80.57	0.55
29	100	120	5.57	85.81	0.62
30	100	150	5.11	86.54	0.79
31	120	0	16.12	54.71	0.60
32	120	30	8.12	66.35	0.49
33	120	60	6.25	79.10	0.43
34	120	90	5.37	86.63	0.41
35	120	120	4.83	91.95	0.40
36	120	150	4.48	89.86	0.39

Table 1. FEA results for the pipes struck at the middle position

No.	D (mm)	p (bar)	W (mm)	F (kN)	E (kJ)
1	22	0	21.71	55.22	0.83
2	22	30	21.61	53.93	0.83
3	22	60	21.50	56.42	0.82
4	22	90	21.41	57.16	0.82
5	22	120	21.31	54.85	0.82
6	22	150	21.24	56.19	0.81
7	42	0	19.20	59.17	0.80
8	42	30	18.56	60.56	0.77
9	42	60	17.95	62.24	0.75

No.	D (mm)	p (bar)	W (mm)	F (kN)	E (kJ)
10	42	90	17.43	63.13	0.74
11	42	120	16.98	64.10	0.73
12	42	150	16.56	64.89	0.73
13	60	0	19.00	61.38	0.76
14	60	30	17.11	65.92	0.71
15	60	60	15.76	69.63	0.68
16	60	90	14.64	72.20	0.67
17	60	120	13.72	73.57	0.67
18	60	150	12.81	76.15	0.68
19	80	0	18.76	60.63	0.74
20	80	30	13.27	68.61	0.69
21	80	60	12.95	75.48	0.65
22	80	90	11.01	78.49	0.63
23	80	120	10.04	81.48	0.61
24	80	150	9.02	84.71	0.60
25	100	0	18.39	58.91	0.72
26	100	30	12.36	68.72	0.63
27	100	60	9.99	79.35	0.57
28	100	90	7.72	84.12	0.54
29	100	120	6.79	86.52	0.52
30	100	150	5.78	89.78	0.51
31	120	0	18.04	54.79	0.68
32	120	30	10.52	68.21	0.58
33	120	60	7.68	78.82	0.50
34	120	90	4.63	89.96	0.46
35	120	120	4.21	101.1	0.42
36	120	150	4.10	101.1	0.42

Table 2. FEA results for the pipes struck at one quarter span position

RESPONSE SURFACE METHOD [2]

In modern industry, RSM is extensively applied in developing, improving, formulating, and optimizing processes. During a design process, such method is used to determine potential influences of several input variables (independent variables) on the performance or quality of the entire system so as to acquire optimized responses from that system. This method has also been extensively applied by the author in optimum design of thin-walled columns in order to optimize their energy absorption capacity during crash analysis [3-8]. In this study, RSM is employed to determine how the internal pressure (p) and outside diameter (D) of the mild-steel pipelines affect their impact response, including impact force (F), permanent deformation (W), and absorbed energy (E).

In this study, the impact response of the pipelines (it can be the impact force, deformation, and absorbed energy) is approximated using a series of the basic functions in a form of

$$\hat{y}(x) = F(p, D), W(p, D), \text{ or } E(p, D) = \sum_{i=1}^n \beta_i \varphi_i(p, D) \quad (1)$$

where n represents the number of basic functions $\varphi_i(p, D)$. In this paper, the polynomials are used to build up these basic functions to formulate F, W, and E.

In Eq. (1), the β_i , known as the regression coefficients, are estimated using the method of least squares. Suppose we have m ($m > n$) observations (obtained from FEA) for the yielded response y_i ($y_1 - y_m$) based on the m sampling design points (p, D)_i, the least squares function is therefore expressed as

$$L = \sum_{i=1}^m \varepsilon_i^2 = \sum_{i=1}^m \left[y_i - \sum_{j=1}^n \beta_j \varphi_j(p, D) \right]^2 \quad (2)$$

where the design points (p, D)_i are selected from the specified design space, ε_i is the error between the response y_i observed at these points, and the RS approximation at that point. Afterwards, the coefficient vector $b = (\beta_1, \beta_2, \dots, \beta_n)$ can be determined by $\partial L / \partial \beta = 0$, which is

$$b = (\Phi^T \Phi)^{-1} \Phi^T y \quad (3)$$

where Φ denotes the matrix consisting of basic functions evaluated using m sampling points, which is

$$\Phi = \begin{bmatrix} \varphi_1(p, D)_1 & \cdots & \varphi_n(p, D)_1 \\ \vdots & \ddots & \vdots \\ \varphi_1(p, D)_m & \cdots & \varphi_n(p, D)_m \end{bmatrix} \quad (4)$$

By substituting Eq. (3) into (1), the response surface model is created and the response functions (F(p, D), W(p, D), and E(p, D)) then can be fully determined.

The accuracy of the developed response surface model can be verified through several techniques. The relative error (RE) between the observed response at those sampling points $y(x)$ and the original response $\hat{y}(x)$ is

$$RE = [\hat{y}(x) - y(x)] / y(x) \quad (5)$$

Other two important properties in evaluating the model's accuracy are the sum of squares of the residuals (SS_E) and the total sum of squares (SS_T), which are

$$SS_E = \sum_{i=1}^m (y_i - \hat{y}_i)^2 \quad (6)$$

$$SS_T = \sum_{i=1}^m (y_i - \bar{y}_i)^2 \quad (7)$$

where \bar{y}_i is the mean value of y_i .

The model's fitness can be evaluated based on the F statistic, coefficient of multiple determination R^2 , adjusted R^2 statistic, and root mean square error (RMSE) respectively, which are calculated as

$$F = \frac{(SS_T - SS_E) / n}{SS_E / (m - n - 1)} \quad (8)$$

$$R^2 = 1 - \frac{SS_E}{SS_T} \quad (9)$$

$$R^2_{adj} = 1 - \frac{m-1}{m-n} (1 - R^2) \quad (10)$$

$$RMSE = \sqrt{\frac{SS_E}{m - n - 1}} \quad (11)$$

According to the classical RSM theory, the larger the values of R^2 and R^2_{adj} , and the smaller the value of RMSE, the better the model fit.

RSM MODELS AND ASSESSMENT

As shown in Tables 1 and 2, six pressures and diameters were selected for modeling and simulation and totally 36 combinations were presented. Thus, in Eqn. (4) the matrix Φ has 36 rows ($m = 36$), which corresponds to the 36 combinations of p and D (No. 1 to 36 in Tables 1 and 2). In this study, quartic polynomial is used as the basic function because it provides the best fitness to the real problems [9]. Thus, the basic functions ϕ_i are terms in a full quartic form, which are 1, p , D , p^2 , pD , D^2 , p^3 , p^2D , pD^2 , D^3 , p^4 , p^3D , p^2D^2 , pD^3 , D^4 . Substituting p and D values into Eqn. (4), a 36×15 matrix Φ then can be created.

Next, response surface models (quartic polynomials) are created for F , W , and E separately. Based on the FEA results listed in Tables 1 and 2, the regression coefficients are determined using Eqn. (3) and then the corresponding quartic polynomial functions are achieved as:

Mid-span impact

$$F(p, D) = 61.6544 - 1.4153D + 0.1107P + 0.0426D^2 - 0.0052DP - 0.0013P^2 - 4.2401 \times 10^{-4}D^3 + 9.1900 \times 10^{-5}D^2P + 3.7256 \times 10^{-5}DP^2 + 5.1727 \times 10^{-6}P^3 + 1.3587 \times 10^{-6}D^4 - 2.2408 \times 10^{-7}D^3P - 2.1514 \times 10^{-7}D^2P^2 - 1.1283 \times 10^{-7}DP^3 - 1.0288 \times 10^{-9}P^4 \quad (12)$$

$$W(p, D) = 45.0506 - 0.4446D + 0.0670P - 0.0047D^2 - 0.0030DP + 0.0002P^2 + 0.0001D^3 - 7.3635D^2P + 2.8224 \times 10^{-5}DP^2 - 1.0382 \times 10^{-5}P^3 - 4.5878 \times 10^{-7}D^4 + 2.8113 \times 10^{-8}D^3P + 5.3156 \times 10^{-8}D^2P^2 - 1.1328 \times 10^{-7}DP^3 + 4.9168 \times 10^{-8}P^4 \quad (13)$$

$$E(p, D) = -0.0071 + 0.0676D + 0.0048P - 0.0017D^2 - 0.0003DP + 6.6842 \times 10^{-6}P^2 + 1.6911 \times 10^{-5}D^3 + 3.5967 \times 10^{-6}D^2P + 4.9025 \times 10^{-7}DP^2 - 5.2068 \times 10^{-8}P^3 - 5.6130 \times 10^{-8}D^4 - 1.7108 \times 10^{-8}D^3P - 4.5308 \times 10^{-10}D^2P^2 - 7.7971 \times 10^{-10}DP^3 + 2.1434 \times 10^{-10}P^4 \quad (14)$$

One quarter-span impact

$$W(p, D) = 27.4686 - 0.3884D - 0.0101P + 0.0068D^2 - 0.0004DP + 0.0009P^2 - 5.5470 \times 10^{-5}D^3 - 3.0335 \times 10^{-5}D^2P + 1.1911 \times 10^{-5}DP^2 - 1.18314 \times 10^{-5}P^3 + 1.6885 \times 10^{-7}D^4 + 9.1578 \times 10^{-8}D^3P + 8.5204 \times 10^{-8}D^2P^2 - 6.3737 \times 10^{-8}DP^3 + 4.5053 \times 10^{-8}P^4 \quad (15)$$

$$F(p, D) = 64.1047 - 0.9443D - 0.0727P + 0.0311D^2 + 0.0038DP + 0.0007P^2 - 0.0003D^3 - 2.3917 \times 10^{-5}D^2P + 9.1220 \times 10^{-6}DP^2 - 1.3172 \times 10^{-5}P^3 + 1.1364 \times 10^{-6}D^4 + 2.2955 \times 10^{-7}D^3P - 3.9789 \times 10^{-8}D^2P^2 - 7.9129 \times 10^{-8}DP^3 + 6.0914 \times 10^{-8}P^4 \quad (16)$$

$$E(p, D) = 0.9443 - 0.0069D + 0.0004P + 0.0001D^2 - 3.4112 \times 10^{-5}DP - 7.2483 \times 10^{-7}P^2 - 8.2700 \times 10^{-7}D^3 - 6.4675 \times 10^{-9}D^2P + 2.0426 \times 10^{-7}DP^2 - 1.06027 \times 10^{-8}P^3 + 2.18127 \times 10^{-9}D^4 - 1.1507 \times 10^{-10}D^3 - 3.0748 \times 10^{-10}D^2P^2 - 1.5731 \times 10^{-10}DP^3 + 4.4457P^4 \quad (17)$$

The approximation of the responses obtained from the response functions and the FEA results are then substituted into Eqns. (6) to (11) to evaluate the fitness of the developed RS models. In those equations $m = 36$ and $n = 15$ (number of basic functions in a full quartic polynomial form). The values of RE , R^2 , R^2_{adj} , and $RMSE$ are calculated and displayed in Table 3. The generated response surfaces with respect to variables pressure and diameter are plotted in Figs. 3 and 4.

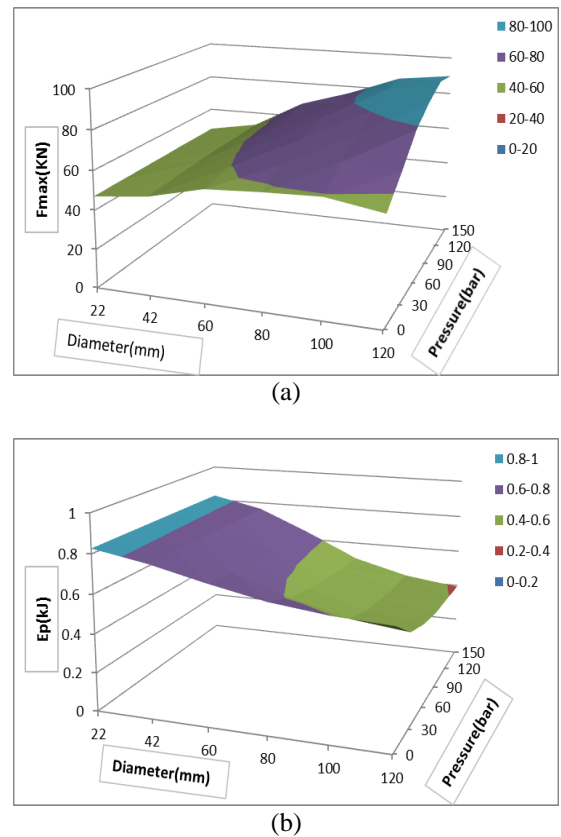
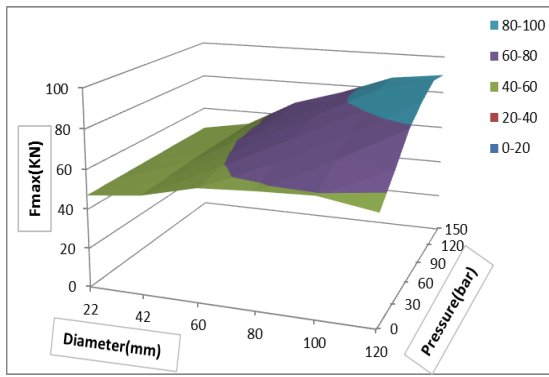
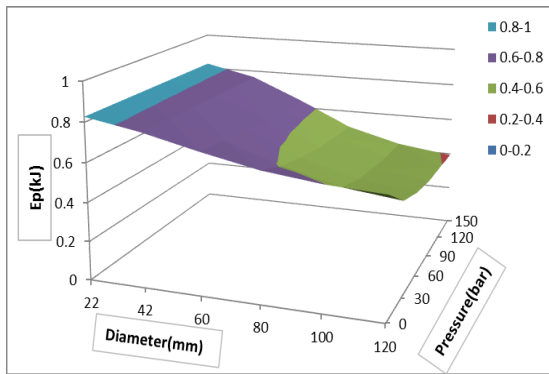


Fig 3. Quartic response surfaces of (a) F ; (b) E under mid-span impact



(a)



(b)

Fig 4. Quartic response surfaces of (a) F_{max} ; (b) E_p under one quarter span impact

From figure 3 and 4, it can be observed that the different impact positions did not largely change the characteristic lateral impact response of the pressurized pipelines. The response surfaces of maximum impact force, and absorbed energy obtained from both impact scenarios showed similar shapes.

Table 3. Evaluation of the developed RS models

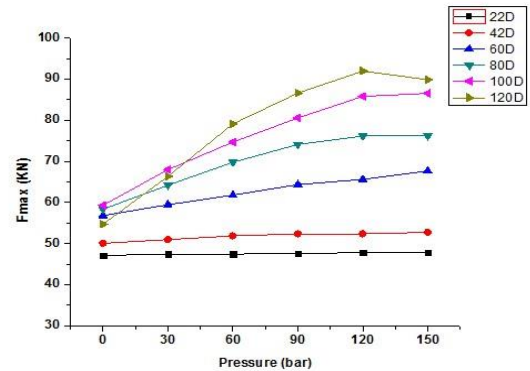
RS model	R^2	R^2_{adj}	RMSE
F mid-span	0.9967	0.9945	1.4838
W mid-span	0.9981	0.9969	0.8091
E mid-span	0.9171	0.8618	0.3027
F one quarter span	0.9933	0.9889	1.4148
W one quarter span	0.9965	0.9942	0.6151
E one quarter span	0.9969	0.9948	0.0123

PARAMETRIC STUDIES

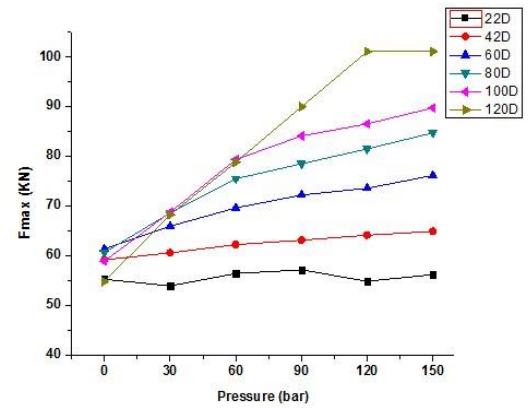
Influence of Internal Pressure

In order to reveal the effects of internal pressure on the pipelines' lateral impact response, as well as validate the accuracy of the developed response surface models, we substitute $D = 22, 42, 60, 80, 100,$ and 120 into Eqns. (12-17) to obtain a series of simplified analytical models with the

internal pressure p as the only variable. Curves are then plotted from those analytical models and compared with the results obtained from FEA simulations. (As displayed in Figs. 5 and 6)

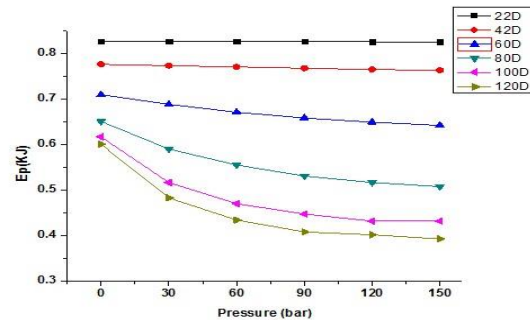


(a)



(b)

Fig 5. Effects of p on maximum impact force, (a) Mid-span impact (b) one quarter span impact



(a)

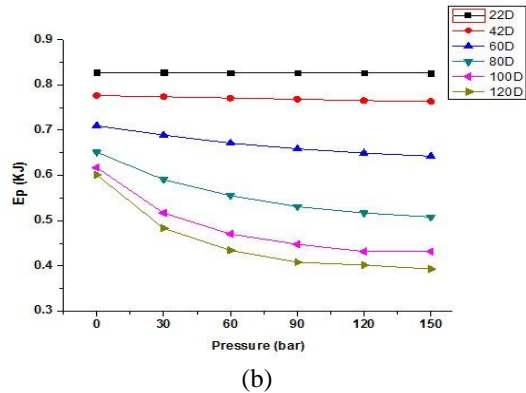
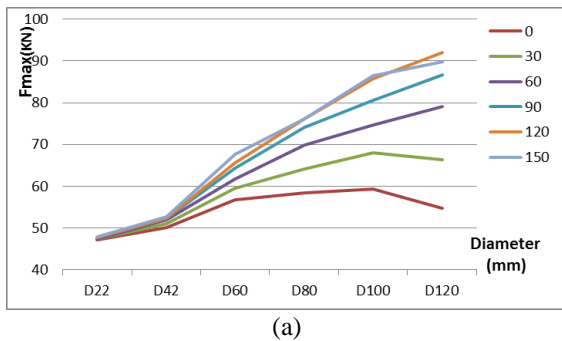


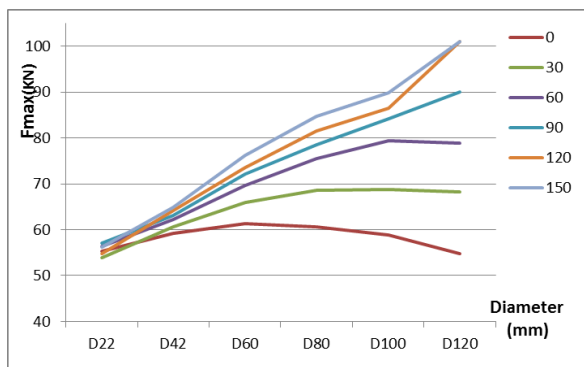
Fig 6. Effects of p on absorbed energy, (a) mid-span impact (b) one quarter span impact

Influence of Outside Diameter

Similarly, in order to study the effects of outside diameter on the pipelines' lateral impact response, $p = 0, 30, 60, 90, 120, 150$ are substituted into Eqns. (12-17) separately to create a series of analytical models with the outside diameter as the only variable. Those analytical models are then compared with the FEA results and the comparison results are shown in Figs. 8 and 9.

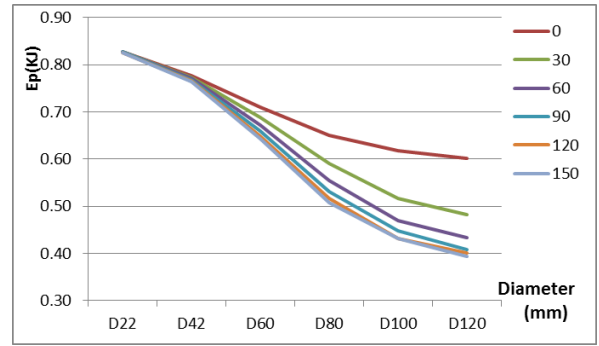


(a)

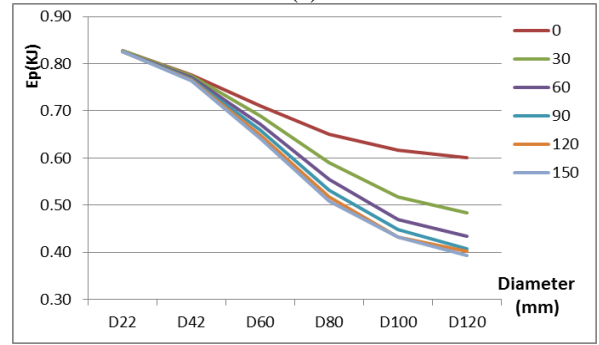


(b)

Fig 7. Effects of D on maximum impact force, (a) Mid-span impact (b) one quarter span impact



(a)



(b)

Fig 8. Effects of D on absorbed energy, (a) Mid-span impact (b) one quarter span impact

Discussion

It seems the influences of internal pressure and diameter on the impact response of those pipelines provide similar tendencies under both mid-position impact and one quarter-position impact (Figs. 5 to 8).

Meanwhile, different impact positions really affect the values of maximum impact force, and absorbed energy. Figs 5(a) and 5(b) discuss that the maximum impact forces yielded during the one quarter-position impact were apparently higher than those generated during the mid-position impact. This is because that the "one quarter position" is closer to fixture and therefore is more rigid than the "middle position". However, as reflected from Figs. 6(a) and 6 (b), the impact energy absorbed during the mid-position impact was slightly lower than that absorbed during the one quarter-position impact.

As for the influences of the internal pressure and outside diameter, Figs 5(a) and 5(b) reveal that when the internal pressure increased, the maximum impact force also increased, even such tendency was not apparent when the outer diameter was low. It is believed that the internal pressure will enhance impact resistance of the pipeline model, therefore leads to higher impact forces. Meanwhile, those figures also tell us that under the same pressure, the pipeline models with larger outside diameter may be subjected to higher impact force.

Figs. 6(a) and 6 (b) show that when the internal pressure increased, the impact energy absorbed by the pipelines decreased (still, such tendency was not that evident for pipelines with a small outside diameter). Similar finding was also

reported in Ng and Shen's work, which were obtained through experiments. Since the internal pressure enhances the rigidity of the pipeline, that way the indenter will rebound at a comparatively high speed after impacting the pipeline and less impact energy will be absorbed by the pipeline. Meanwhile, from both figures it is observed that the absorbed impact energy decreased when the outside diameter increased.

Those effects of outside diameter on the pipelines' lateral impact response are reflected in Figs. 7 (a) and 7 (b) as well as Figs. 8 (a) and 8 (b). Different impact position did affect maximum impact force even those curves seem similar and have same tendency as shown in Figs 7 (a) and 7 (b). The pipeline with impact "one quarter position" is near to boundary condition and therefore is more rigid than the "middle position". Those figures also reveal that outside diameter increased while the maximum impact force increasing as well. The slope of each curve is different and gradually increased. It is reasonable to have larger value of maximum impact force with higher internal pressure which could increase the impact resistance of pipeline model.

Figs. 8 (a) and 8 (b) are used to illustrate influences of diameter on the impact response of those pipelines under different impact position scenarios which is center position and quarter span separately. It is obviously to determine diameter increased as impact energy absorbed energy decreased. With increasing of diameter and internal pressure, there will have more resistance force to avoid deformation and weaker ability to absorbed energy.

CONCLUSIONS

This paper provides a combined computational and analytical study to investigate the lateral impact behavior of pressurized pipelines and inspect all the parameters such as the outside diameters and internal pressures affect such behavior.

In this study, the effects of the diameter and pressure on maximum force (F), permanent deformation (W), and absorbed energy (E) are illustrated through analyzing those functions which is listed above.

1. In this study, quartic polynomial is built and used as the basic function and provides the best fitness. Therefore basic functions ϕ_i are terms in a full quartic form, which are 1, p, D, p², pD, D², p³, p²D, pD², D³, p⁴, p³D, p²D², pD³, D⁴.) A 36×15 matrix Φ is created in order to determine the influence.
2. Response surfaces are plotted based on the generated quartic polynomial functions and the quality (accuracy) of those functions are verified through several techniques.
3. When the internal pressure increases, the maximum impact force increases, the maximum transverse displacement decreases, and the absorbed impact energy also decreases.
4. When the outside diameter increases, the maximum impact force increases, the maximum transverse displacement decreases, and the absorbed impact energy decreases also.

This paper could be used as a guidance to determine the suitable polynomial functions which are verified through statistic methods. With the purpose of predication the influences of internal pressure and diameter on the impact response of those pipelines under both mid-position impact and one quarter-position impact, a quartic polynomial is chosen to represent those models and a group of detailed 2D curves are selected to reveal the relationship between the parameters. However in order to get a fully explanation the influences of the internal pressure and outside diameter found from this study, a complete experimental analysis is needed to be as a positive comparison.

ACKNOWLEDGMENTS

This study was sponsored by Louisiana Board of Regents (LA BoR) with contract No. LEQSF(2012-15)-RD-A-28. The financial support is greatly appreciated.

REFERENCES

- [1] B.N. Leis, R.B. Francini, R. Mohan, D.L. Rudland and R.J. Olson, "Pressure-displacement behavior of transmission pipelines under outside forces towards a serviceability criterion for mechanical damage", Proceedings of the 8th International Offshore and Polar Engineering Conference, Canada, 1998, 60-67.
- [2] H. Oktem, T. Erzurumlu and H. Kurtaran, "Application of response surface methodology in the optimization of cutting conditions for surface roughness", *Journal of Materials Processing Technology*, 170, 2005, 11-16.
- [3] Y.-C. Liu, "Optimum design of thin-walled box section beams for crashworthiness analysis", *Finite Elements in Analysis and Design*, 44(3), 2008, 139-147.
- [4] Y.-C. Liu, "Design optimization of tapered thin-walled square tubes", *International Journal of Crashworthiness*, 13(5), 2008, 543-550.
- [5] Y.-C. Liu, "Crashworthiness design of multicorner thin-walled columns", *Thin-Walled Structures*, 46(12), 2008, 1329-1337.
- [6] Y.-C. Liu, "Crashworthiness design of thin-walled curved beams with box and channel cross sections", *International Journal of Crashworthiness*, 15(4), 2010, 413-423.
- [7] Y.-C. Liu, "Thin-walled curved hexagonal beams in crashes – FEA and design", *International Journal of Crashworthiness*, 15(2), 2010, 151-159.
- [8] Y.-C. Liu, "Optimization of the crushing performance of tubular structures", *HKIE (The Hong Kong Institution of Engineers) Transactions*, 17(1), 2010, 16-25.
- [9] S.-J. Hou, Q. Li, S.-Y. Long, X.-J. Yang and W. Li, "Design optimization of regular hexagonal thin-walled columns with crashworthiness criteria", *Finite Elements in Analysis and Design*, 43, 2007, 555-565.